SHOCK ANNEALING CHARACTERIZATION OF MILLER RANGE 090031 UREILITE USING RAMAN SPECTROSCOPY AND ENERGY-DISPERSIVE X-RAY SPECTROSCOPY. P.F. Silaghi[1], J.M. Trigo-Rodríguez[1], M. Martínez-Jiménez[1], N. Mestres[2].[1]Meteorites, Minor Bodies and Planetary Science Group, Institute of Space Sciences (CSIC-IEEC). Campus UAB, Carrer de Can Magrans s/n, 08193 Cerdanyola del Vallés, Barcelona, Spain. trigo@ice.csic.es. [2]Institut de Ciència del Materials de Barcelona (ICMAB/CSIC), Campus UAB, 08093 Bellaterra (Barcelona) Spain.

Introduction: Ureilites are the second largest group of achondrite meteorites, being mainly formed by olivine and low-Ca pyroxene [1-3]. A plausible scenario for the formation of the ureilite parent body (UPB), is that the UPB accreted, and began its differentiation soon after its accretion. Once the differentiation ended, the UPB suffered intense impact events which disrupted it and then ureilite daughter bodies (UDB) were formed. These UDB followed different evolutionary pathways, so they evolved separately until producing the diversified ureilitic materials arrived to Earth [4]. Other models proposed for describing the origin of these meteorites are that they may be partial melt residues, igneous cumulates, nebular condensates, or paracumulates [5]. As a consequence of their complex evolution, ureilites have experienced different shock degrees, from moderate to severe, most of them being monomict rocks, while a few are polymict breccias and at least one has been identified as a dimict breccia [1, 4, 5]. Our ureilite specimen, Miller Range 090031 (hereafter MIL 090031), was found in Antarctica in 2009. In thin section this meteorite is formed by an aggregate of large olivine and pyroxene grains. Olivine grains are surrounded by carbon-rich amorphous material with traces of metal, and have been mosaicized by shock. The olivine grains exhibit reduction rims, with minor pigeonite content having a blotchy appearance.

Technical procedure: One thin section of MIL 090031 provided by NASA was studied. High-resolution mosaics of the sections were created from separate 50X images taken with a Zeiss Scope petrographic microscope. The mosaic allowed us to establish points of interest to be characterized by micro-Raman. We also made SEM/EDX studies of the regions studied with micro-Raman.

Micro-Raman study. Several micro-Raman spectra were taken in backscattering geometry at room temperature using 5145 Å line of Argon-ion laser with a Jobin-Yvon T-64000 Raman spectrometer attached to an Olympus microscope and equipped with a liquid-nitrogen-cooled CCD detector. The Raman points are marked in blue in Figure 1. Their lateral spatial resolution was ~1 μm and the laser power onto the sample was kept below 0.5 mW to avoid degradation due to sample overheating. The Raman spectrometer provided spectra in a working range between 100 and 1.300 cm^{-1}. Finally, our study was complemented using SEM/EDX techniques with an *Evo Zeiss* SEM working at 20 kV. The sample was not coated in order to allow studying its C content, so it was analyzed under variable pressure with a detection error of ~ 1%.

Results and discussion: the matrix of the MIL 090031, is rich in forsterite (Mg_2SiO_4) which has been altered by shock as we can see in its Raman spectra, (see Fig.2). Its matrix also contains amorphous carbon and veins which are filled with iron-oxides and probably hematite which is very altered as its Raman spectra shows (see Fig. 2). Nickel in low amounts is also found at some locations in the veins, and may indicate that iron-nickel oxides were present, and after altered. Now, they are only present as iron-oxides. Dark and opaque nodules are probably consequence of impact heating, characterized by having graphitized carbon in the SEM/EDX analyses. Due to the amorphous nature of these nodules we have not found a clear Raman signature, probably consistent with an extensive disorder in those nodules produced by shock and subsequent thermal processing [7-8]. Imbedded in the matrix we found mm-sized olivine crystals with many fractures, and some of them being probably partially filled with iron-oxides. Besides the coarse olivine crystals, also pyroxene silicate crystals from the enstatite ($MgSiO_3$) - ferrosilite ($FeSiO_3$) series can be found, most of them with amorphous carbon filling their fractures (Fig. 3).

Conclusions: it is likely that MIL 090031 suffered extensive shock by successive impacts as indicates by Raman spectra, and other classic features like e.g. the planar deformation structures in olivine and pyroxene, found using a petrographic microscope. By using that instrument, it is also possible to identify dendritic growth in olivine which in itself is a clear shock signature. Additionally we also found undulatory extinction and simple twinning in some pyroxene crystals. In view of all these signatures, including the planar deformation structures in olivine, and the opaque shock

veins, this sample can be classified as a S5 stage of shock, indicating that it was shocked at least to 30-35 GPa [6].

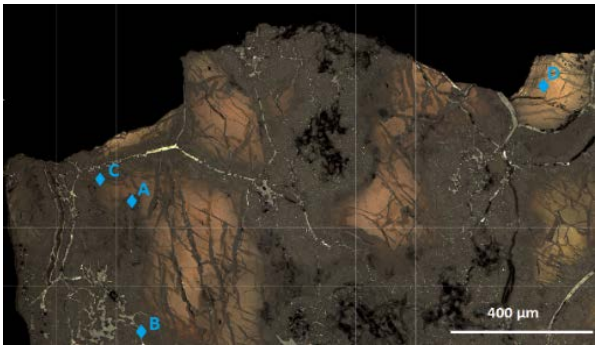

Figure 1. Region of MIL 090031 section in RL showing the Raman points shown in Fig. 2

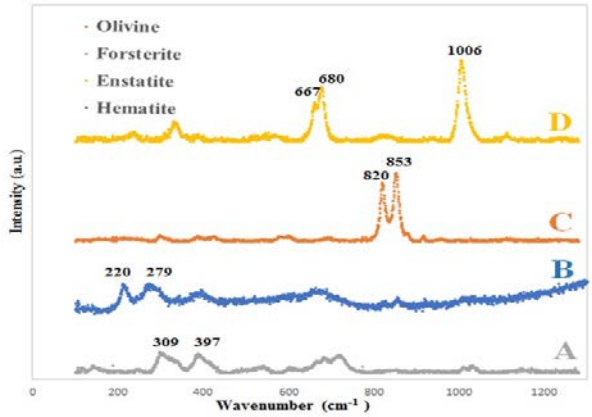

Figure 2. Raman spectra of the olivine (C), forsterite (A), enstatite (D) and hematite (B) points in Fig. 1.

Acknowledgments: We acknowledge the funding support received from the Spanish Ministry (project AYA2011-26522). We thank the NASA Meteorite Working Group, and Johnson Space Science curators for providing the section analyzed here.

References: [1] Bischoff A., et al. (2006) In *MESSII*, D.S. Lauretta, and H. Y. McSween (Eds.), Univ. Arizona, pp. 679-711. [2] Goodrich C.E. et al. (2004) *Chemie der Erde*, 64, 283 [3] Weisberg M.K., et al. (2006) In *MESSII*, D.S. Lauretta, and H.Y. McSween (Eds.), Univ. Arizona, pp.19-52. [4] Goodrich C.A. et al. (2014) *Meteoritics & Planet. Sci.*, 50, 782-809. [5] Rubin A.E. (1988) *Meteoritics*, 23, 333-337. [6] Stöffler D. et al. (1991) *Geochim. et Cosmoch. Acta*, 55, 3845-3867. [7] Wang A. et al. (1998) LPSC Conference, LPI, abstract #1819. [8] A. Wright and J. Parnell (2007) LPSC Conference, LPI, abstract #1228.

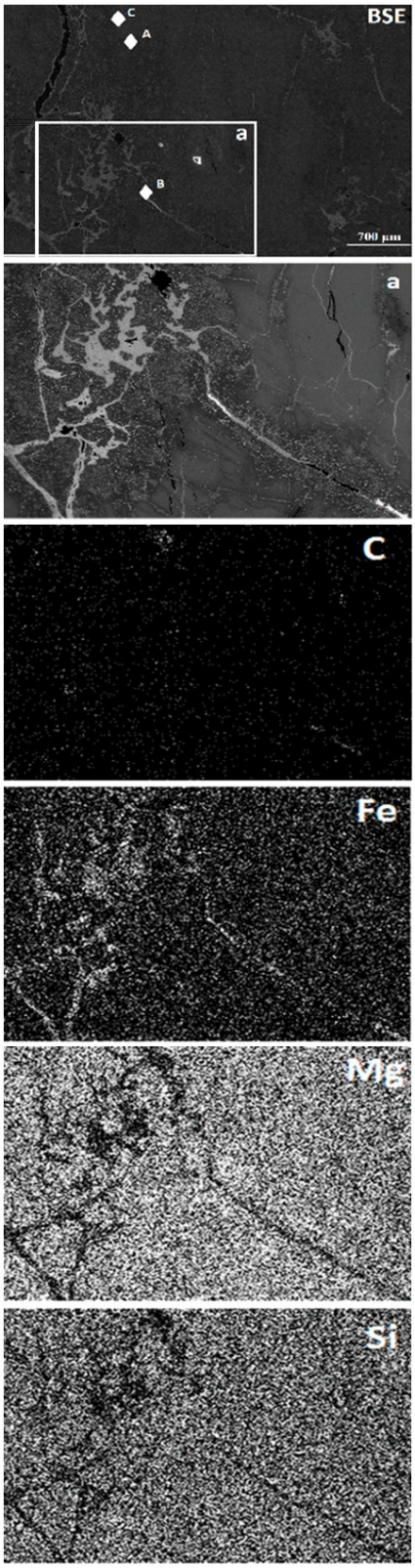

Figure 3. Back-scattered electron (BSE) images and four EDX elemental maps of the inset zone for carbon, iron, magnesium, and silicon.